Theoretical and experimental investigation of the optical properties of poly(paraphenylene): Evidence of chain-length distribution

E. Mulazzi and A. Ripamonti
Dipartimento di Fisica dell'Università di Milano and Istituto Nazionale di Fisica della Materia, v. Celoria 16, Milano 20133 Italy

L. Athouël, J. Wery, and S. Lefrant
Laboratoire de Physique Cristalline, Institut des Matériaux de Nantes, 2 rue de la Houssinière, BP 32229, 44322 Nantes Cedex 03, France

(Received 16 April 2001; published 6 February 2002)

We present an experimental and theoretical investigation of the optical absorption and Raman spectra of electropolymerized poly(para-phenylene) (PPP) and related oligomers. Experimental data include also the photoluminescence spectra of all these polymeric compounds. Theoretical calculations of the band shapes of both optical absorption and Raman spectra of PPP are reported, based on the spectroscopic properties of known polymeric chains of different lengths. Such calculations have been carried out by taking into account the electronic levels involved in the optical transitions, the most intense Raman active vibrational modes, and the interaction between these vibrations and the electronic states considered for the different conjugation lengths. We show that in order to account theoretically for the optical experimental data of PPP samples issued by different synthesis, a distribution of conjugated segments of various lengths must be included in the calculations.

DOI: 10.1103/PhysRevB.65.085204 PACS number(s): 78.30.Jw, 78.66.Qn

I. INTRODUCTION

In a recent paper,[1] we proved that a distribution of conjugated segment lengths in poly-phenylene vinylene (PPV) is needed in order to calculate the optical absorption and the Raman spectra and their changes according to samples issued by different synthesis, in good agreement with the experimental data. The theoretical model used in this reference was applied before in polyacetylene[2] and derivative polymers,[3,4] in order to determine the optical band-shape changes in photoinduced infrared absorption, optical absorption, and Raman scattering, and the frequency shift of their maxima observed in different samples. In addition, the Raman band modifications were also investigated as a function of the excitation wavelength. This was accomplished by taking into account the dependence on the conjugation length of the segments of the electronic transition energies and the vibrational frequency values of the normal modes involved.

In the case of conjugated polymers with aromatic rings, no vibrational frequency shift is observed in the whole range of laser exitations,[5] whereas dramatic changes in the relative intensities of specific Raman bands are detected. This behavior can be readily explored because the Raman bands of these polymeric systems are narrow and the assignments[5] are clearly identified. Another specific advantage comes from the possibility of using oligomers of known lengths as references for both absorption and Raman spectra.

The determination of conjugation length distribution in conjugated polymers is of primary importance in order to optimize this type of materials to be used in electronic devices such as LED's (light-emitting diodes), etc. In this work, we present results obtained in poly-paraphenylene (hereafter referred to as PPP) which also has potential applications in LED's, by providing a blue range emission. Let's recall that in the case of PPP, different synthesis methods have been developed, leading to so-called ''Kovacic'' [6] and ''Yamamoto'' [7] samples. In the present study we mostly use electropolymerized material whose synthesis was proposed later[8] (hereafter referred to as standard PPP). In Sec. II, we present experimental data for absorption, Raman scattering, and luminescence of electropolymerized PPP, and the data are compared to those obtained with PPP synthesized by different methods. We also present spectroscopic characteristics, including absorption and Raman features, of the phenylene oligomers from biphenyl to octophenyl. These data are needed in order to give a coherent interpretation of the spectroscopic features of standard PPP. In Sec. III, calculations of the absorption spectra and the relative intensities of the Raman bands of the oligomers and of PPP obtained with different synthesis are presented. Furthermore in that section, the relative Raman band intensities are also studied as functions of the excitation wavelengths. The calculations of the optical features of PPP are performed by introducing a distribution of conjugation lengths characterized by different number of phenyl rings. In Sec. IV, we discuss the results, and we stress the importance of such a distribution to understand the electronic and optical properties of PPP.

II. EXPERIMENTAL RESULTS

A. Experimental details

Biphenyl (Φ_2), terphenyl (Φ_3), and quaterphenyl (Φ_4) oligomers were provided by Aldrich and used in powder form. Sexiphenyl, octophenyl, and PPP were synthesized by using an electrochemical procedure as discussed previously.[9] Samples were used in powder form or processed in thin films depending on the type of experiment. Absorption experiments were carried out on a 2300 Cary model Spectrometer. Raman spectra were recorded with a T64000 Jobin Yvon spectrometer equipped with a cooled CCD detector, when using excitation laser wavelengths in the range 351.1–676

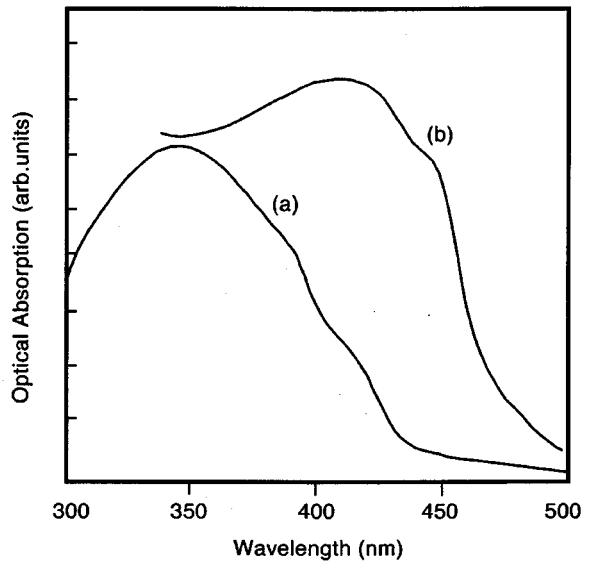

FIG. 1. Optical absorption spectra of PPP thin films recorded at room temperature (RT): (a) standard electropolymerized PPP; (b) improved electropolymerized PPP.

nm. Raman experiments with the 1064-nm excitation were carried out with a Fourier transform Raman Brücker RFS100. Raman spectra were taken with a 2 cm^{-1} resolution with excitation in the red range ($\lambda_L = 1064$ mm and 676 nm), and 4 cm^{-1} with other wavelengths. Photoluminescence data were obtained with a monocanal J. Y. Spectrometer HG2S, with a cooled Hamamatsu photomultiplier as light detector.

B. Absorption and luminescence spectra

In Figs. 1(a) and 1(b), we present the UV visible optical absorption curves of two different electropolymerized PPP samples. Figure 1(a) is the absorption of the- so called ''standard'' PPP, which is used most of the time in spectroscopic investigations. Conversely, Fig. 1(b) is the absorption of an improved PPP sample which is rather difficult to reproduce due to uncontrolled synthesis conditions. Note that the overall shape of Fig. 1(b) is redshifted compared to Fig. 1(a). In particular, the maximum recorded at 388 nm in Fig. 1(b) is at 341 nm for Fig. 1(a). This change in the maximum positions shows that Fig. 1(b) is characteristic of a PPP sample containing on-average, longer conjugated segments with respect to the ''standard'' one. This is evidence that the electropolymerization method could be optimized.

In Fig. 2 we show the optical absorption spectra of the different PPP oligomers. Spectra of Φ_2, Φ_3 and Φ_4 [Figs. 2(a), 2(b), and 2(c)] are taken from Ref. 10. Let us note that a redshift of the overall band shapes is observed, going Fig. 2(a) to Fig. 2(f). In particular in Φ_6 the apparent maximum is peaked at 318 nm with at least one weak shoulder on the low-energy side of the band. This is presumably related to the vibronic structure observed at 4 K in Φ_6 processed in thin film (see Ref. 11). In the case of Φ_8 we may note that the peak maximum is not redshifted, compared to that of the

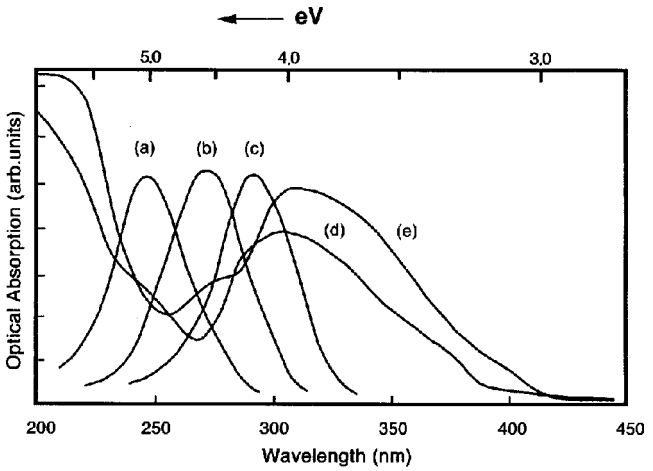

FIG. 2. Optical absorption spectra of PPP oligomers recorded at RT [(a), (b) and (c) are Φ_2, Φ_3, and Φ_4, respectively] in cyclohexane solvent; (d) and (e) Φ_6, and Φ_8 thin films, respectively.

absorption band of Φ_6. Furthermore, the high-energy side of the band exhibits a significant component. This can be interpreted by a mixture of Φ_8 with shorter oligophenyls, which presumably could not be eliminated after the synthesis.

In Fig. 3 we show the photoluminescence data on the complete series of oligomers and electropolymerized PPP. The results for Φ_2, Φ_3, and Φ_4 were taken from Ref. 10, whereas those for Φ_6, Φ_8, and PPP were recorded in the Laboratoire de Physique Cristalline at the Institut des Matériaux de Nantes. The experiments were performed at 77 K. As expected, the structured emission bands are shifted to the red energy range going from Figs. 3(a) to 3(f), as a proof of the segment length dependence of the optical properties of such materials.

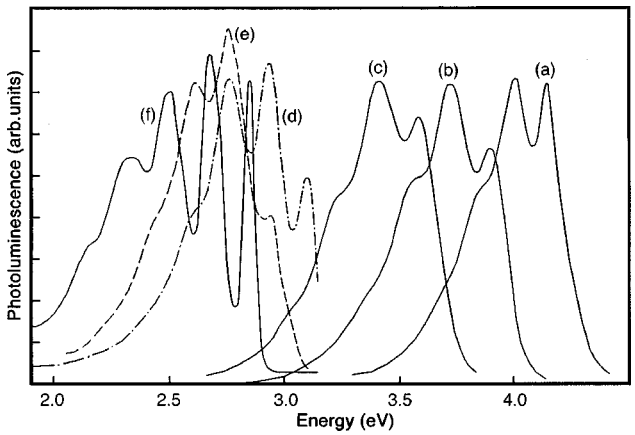

FIG. 3. Photoluminescence spectra of PPP oligomers and standard electropolymerized PPP excited at different excitation wavelengths λ_L: (a) Φ_2 at RT with $\lambda_L = 253.7$ nm; (b) Φ_3 at RT with $\lambda_L = 303$ nm; (c) Φ_4 at RT with $\lambda_L = 313$ nm; (d), (e), and (f) Φ_6, Φ_8, and standard electropolymerized PPP, respectively, at $T = 77$ K with $\lambda_L = 335$ nm, Φ_2, Φ_3, and Φ_4 and oligomers were studied in cyclohexane solvent. Φ_6, Φ_8, and standard electropolymerized PPP were prepared in thin films.

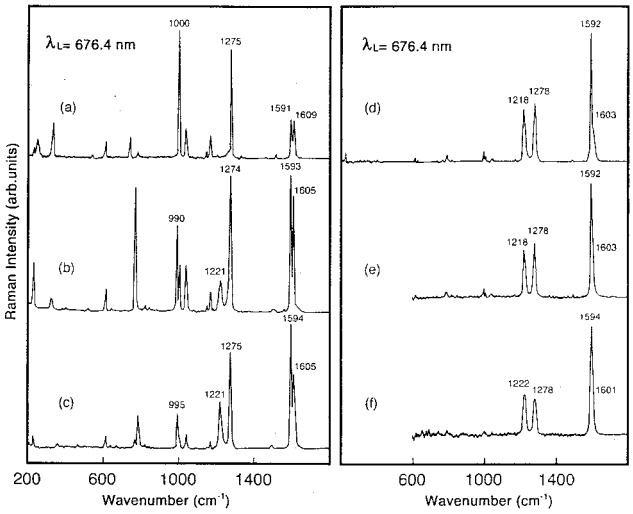

FIG. 4. Raman spectra of PPP oligomers recorded at RT and with an excitation wavelength $\lambda_L = 676.4$ nm: (a), (b), and (c) Φ_2, Φ_3, and Φ_4, respectively; (d) Φ_6 pellet; (e) Φ_6 thin film; and (f) Φ_8, thin film deposited on a glass substrate. Φ_2, Φ_3, and Φ_4 oligomers were studied in compacted pellets.

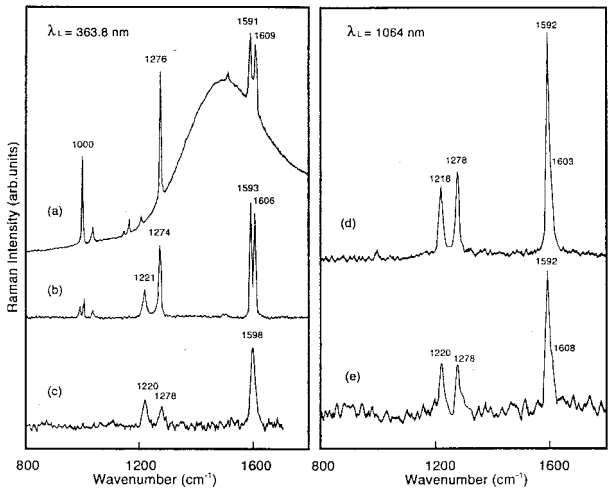

FIG. 5. Raman spectra of PPP oligomers recorded at RT: (a), (b), and (c) Φ_2 pellet, Φ_3 pellet and Φ_8 thin film, respectively, with $\lambda_L = 363.8$ nm; (d) and (e) Φ_6 and Φ_8 thin films, respectively, with $\lambda_L = 1064$ nm.

C. Raman spectra

Raman spectra of PPP oligomers recorded at room temperature (RT) are presented in Figs. 4 and 5 for different excitation wavelengths, chosen in order to avoid the photoluminescence signal when present. For this reason Raman spectra of all oligomers were recorded with $\lambda_L = 676$ nm. For other excitation wavelengths, the choice of specific oligomers were restricted to Φ_2, Φ_3, Φ_8 in the near UV ($\lambda_L = 363$ nm) and to Φ_6 and Φ_8 for $\lambda_L = 1064$ nm. Note that Φ_2, Φ_3, and Φ_4 were studied as compacted pallets, Φ_6 in both powder and thin film and Φ_8 in thin film. The choice in Fig. 4 to show the Raman scattering data from Φ_6 in both powder form and a thin film was determined in order to prove that morphology does not significantly influence the intensity of the Raman bands of the two spectra.

All the oligomers were studied extensively in Raman spectroscopy by many authors (see Refs. 12–16) and the assignment of the Raman bands was given in different references.[12,17–19] In Table I, we collect the frequencies of the main vibrational Raman modes together with their assignment. It can be observed that, whatever the length of the oligomer, the frequencies of the Raman-active modes do not vary. Conversely, from Figs. 4 and 5 one observes that the relative intensity of the Raman bands, whose frequencies at the maximum are listed above, are drastically dependent on the number of phenyl rings. In particular the intensity ratio of I_{1280}/I_{1220} is going from ~30 in Φ_2 to ~1.1 in Φ_6 and to ~0.75 in Φ_8. The change in this ratio was used in the past to evaluate the effective conjugation lengths in PPP polymers qualitatively.[12] It must be noted that the intensity ratio I_{1600}/I_{1280} also exhibits a significant change as the number of the phenyl rings increases. (I_{1600} means the intensity of the highest frequency Raman band of PPP and oligomers we consider in this paper, around 1600 cm^{-1}). This ratio goes from ~1.2 in Φ_2 to 2.5 in Φ_8. This can be used as an additional probe of the determination of the effective conjugation length in PPP polymers. Since the absorption of all the oligomers lies in the near-UV range and out of the domain of the excitation light frequencies investigated in Raman scattering, the slight changes in the intensity ratios recorded in the Raman spectra, as a function of the laser light, are considered negligible in our investigation.

The Raman features of electropolymerized ''standard'' PPP as a function of the excitation wavelengths are shown in

TABLE I. Assignments of the most intense Raman active vibrational modes of the oligophenyls Φ_2, Φ_4, Φ_6, and Φ_8 and of PPP. All the frequencies are given in cm^{-1}.

f	Frequency ω_f	Φ_2	Φ_3	Φ_4	Φ_6	Φ_8	PPP	Main assignment
1	ω_1		1221	1216	1218	1220	1222	C-H bending mode
2	ω_2	1272	1272	1277	1277	1277	1281	Interring stretching mode
3	ω_3	1596 1605	1596 1606	1596	1592	1593	1593	Intraring C-C stretching mode

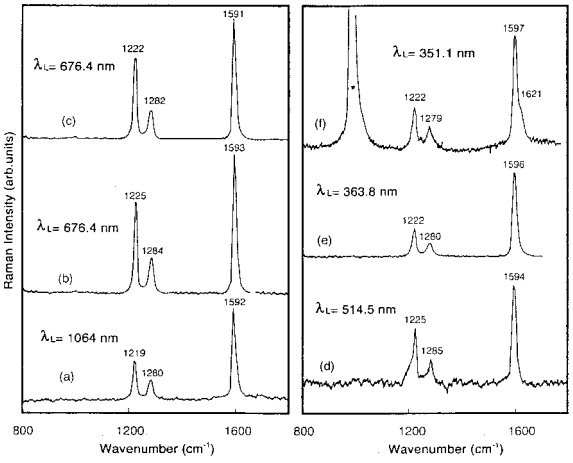

FIG. 6. Raman spectra of standard electropolymerized PPP at RT and for different excitation wavelengths (a) $\lambda_L = 1064$ nm, (b) and (c) $\lambda_L = 676.4$ nm, (d) $\lambda_L = 514.5$ nm, (e) $\lambda_L = 363.8$ nm, and (f) $\lambda_L = 351.1$ nm. Standard electropolymerized PPP was a thin film in all these cases except for case (c), where PPP was a compacted pellet. The asterisk indicates a plasma line from the argon laser.

Fig. 6. The domain of the investigation ranges from $\lambda_L = 1064$ to 351.1 nm. The values and the assignment of the frequencies of the main vibrational Raman active modes of PPP are given in Table I. From these data one can derive that the intensity ratios I_{1280}/I_{1220} and I_{1600}/I_{1280} change with the excitation light wavelength. In particular I_{1280}/I_{1220} varies from the value of 0.52 for $\lambda_L = 1064$ nm to 0.38 for $\lambda_L = 514.5$ nm. For $\lambda_L = 363$ nm, this ratio is found to be 0.5, larger than the value at $\lambda_L = 514.5$ nm. This is an indication that segments of intermediate effective conjugation length are present in the sample and their vibrational modes provide a substantial contribution to the Raman scattering. The intensity ratio (I_{1600}/I_{1280}) variation with the excitation light wavelengths agrees well with this hypothesis. Furthermore, note that in the spectra recorded with UV excitation, especially with $\lambda_L = 351.1$ nm [Fig. 6(f)], a shoulder at 1621 cm^{-1} is observed. This could be an additional indication that short segments make some contribution to the Raman scattering, as it can be deduced from investigation of the oligomers presented in Figs. 4 and 5.

In Fig. 7 we show also the Raman features of electropolymerized PPP, issued from another synthesis with respect to the previous ''standard'' sample, in order to compare the intensity ratios with those determined from Figs. 6. As a matter of fact, a drastic change with respect to the standard PPP case is found with $\lambda_L = 351.1$ nm, where the intensity ratios are $I_{1280}/I_{1220} \sim 1$ and $I_{1600}/I_{1280} \sim 3.5$. This behavior is haracteristic of higher concentration of shorter conjugated segments in the sample, as compared to the standard PPP. This is corroborated by a more pronounced contribution at the high-frequency side of the 1598-cm^{-1} band, as discussed for standard PPP.

The Raman-scattering data shown in Figs. 4–7 put another important point into evidence: the couplings between neighboring segments, if any, are not detectable in the Raman-scattering spectra. In fact no modification (in shape and position) is observed for the Raman bands in the spectra from thin films and powder form of the same compound (oligomer or polymer)

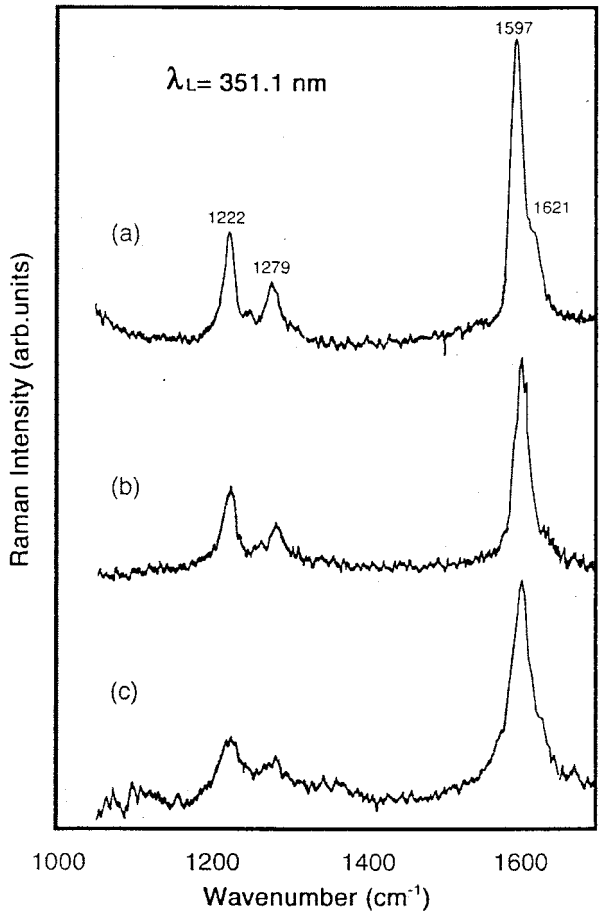

FIG. 7. Raman spectra of electropolymerized PPP issued from different synthesis, in thin films, recorded at RT and with $\lambda_L = 351.1$ nm: (a) standard electropolymerization, (b) Kovacic method, and (c) Fauvarque method.

III. THEORETICAL RESULTS

We have performed calculations of the band shapes observed in the optical-absorption spectra of electropolymerized PPP samples issued by different methods of synthesis (the standard method and the improved one) and of its related oligophenyls. In addition, for the same polymeric compounds, we have evaluated the relative intensities and the shapes of the Raman scattering bands due to the C-C stretching modes and C-H bending modes whose frequencies and assignments are listed in Table I. These calculations have been performed by using a model in which both the optical absorption and the Raman-scattering response functions are evaluated in terms of the same formalism. This model was already shown, discussed, and used in Refs. 1 and 2 in order to check its full potentiality in the calculation of the optical properties of trans $(CH)_x$ and PPV, respectively. The major

TABLE II. Values of Ω_n, $S_{f,n}$, and γ_n used in calculations.

n	2	3	4	5	6	7	8	9–15
Ω_n (eV)	4.6	4.0	3.8	3.62	3.51	3.42	3.3	3.0
S_{1n}	0.05	0.5	0.8	0.8	1.0	1.0	1.3	1.9
S_{2n}	2.4	1.7	1.7	1.7	1.3	1.3	1.2	1.0
S_{3n}	1.1	1.7	1.9	1.9	2.0	2.0	2.6	3.3
γ_n (eV)	0.23	0.25	0.22	0.22	0.21	0.21	0.2	0.1

purpose of these calculations is to show that the absorption and Raman-scattering band shapes of electropolymerized PPP are well interpreted in terms of the contributions of the effective conjugation lengths weighted by a distribution of conjugated segments. Moreover, the change of the relative intensities of the Raman bands as a function of the laser wavelengths, as experimentally observed, can be interpreted in a straightforward way for the electropolymerized PPP samples obtained from different synthesis, on the basis of this model. In fact the observed intensity changes of the Raman bands can be explained only by taking into account that the incident laser wavelengths, going from the red to the near ultraviolet regions, are in resonance with electronic transitions of different effective conjugation lengths.

In order to calculate the optical absorption band shapes and their intensities for the different oligomers whose number of repeating units are indicated by n (for the oligomers considered here, $n=2-15$), we use the following function $I(\Omega,n)$ (Refs. 1 and 2) given in Eq. (1):

$$I(\Omega,n)=|M_n|^2\left\{\sum_{j=0}^{2}\sum_{f=1}^{3}\exp\left[-\sum_{f=1}^{3}S_{f,n}\right]\frac{(S_{f,n})^j}{j!}\times\frac{\gamma_n}{(\Omega-\Omega_n-j\omega_f)^2+\gamma_n^2}\right\}. \quad (1)$$

M_n is the electric dipole moment intensity for the electronic transition of each oligomer with n phenyl rings from the ground state to a $1B_u$ excited state whose frequency is indicated by Ω_n. M_n and Ω_n have been evaluated as in Ref. 1, and the values of Ω_n, as function of n, are listed in Table II. Note that the values of all the physical quantities listed in Table II do not change when referring to conjugation lengths with n going from 9 to 15. In Table II we give also $S_{f,n}$, which are the contributions to the total Huang-Rhys factors S_n, coming from each vibrational mode (labeled by f) interacting with the electronic excited states $1B_u$ of every oligomer with n phenyl rings ($S_n=\Sigma_{f=1}^{3}S_{f,n}$). These contributions are related to the change of the electron vibrational couplings with respect to the ground state for each n and for each vibrational mode f we consider here ($f=1-3$), and whose frequency is indicated by ω_f. In the evaluations presented here we do not take any change of ω_f with n into account and we will consider only the values listed for PPP in Table I.

The values of $S_{f,n}$ have been determined as in Ref. 1, and, as can be noted from Table II, they change as a function of f and n with different trends. In fact, since in all three couplings excited electronic states are involved, the higher degree of planarity of the system with n is felt in a stronger way in these states, due to a larger extension of their wave functions with respect to the ground-state functions. This fact, together with the decreasing localization of the $1B_u$ states with n, therefore plays a major role in the changing trend of the couplings $S_{f,n}$ with n. In fact $S_{2,n}$, which is related to the linear interaction between the interring C-C single bond and the electronic (ground and excited) states, is decreasing with n since this coupling is becoming less intense with the increasing planarity of the system with n.[20] Contrary to this trend, $S_{1,n}$ and $S_{3,n}$ which are related to the linear electron vibration interaction of the C-H bending mode and the intraring C-C stretching mode, respectively, are increasing with n, because of the higher degree of planarity of the system and of the decreasing localization of the excited states with n.

In Fig. 8 we show the calculated absorption band shapes for the Φ_4 and Φ_6 oligomers using Eq. (1). Good agreement is found from the comparison between the experimental data shown in Fig. 2 and the band shapes of Fig. 8.

In order to calculate the optical absorption band shape $I(\Omega)$ of PPP, we use the following equation:

$$I(\Omega)=\sum_{n=2}^{15}I(\Omega,n)\times P_n \quad (2)$$

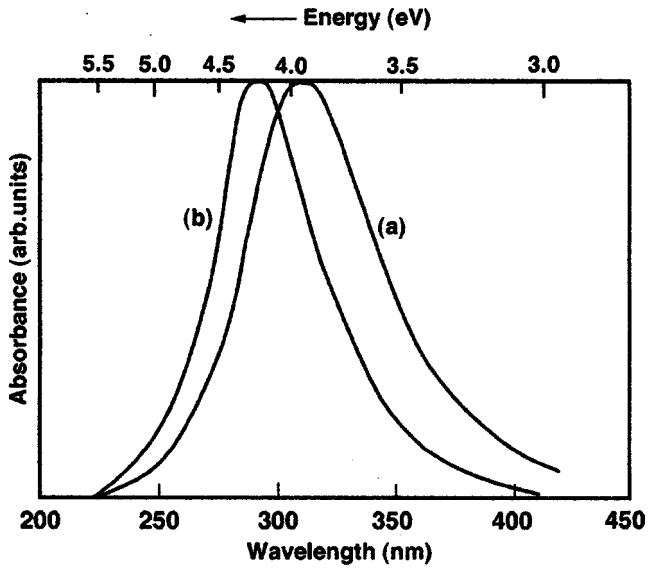

FIG. 8. Calculated absorption curves for the oligomers Φ_4 and Φ_6 using Eq. (1) and the parameter values given in Table II: (a) Φ_6 and (b) Φ_4.

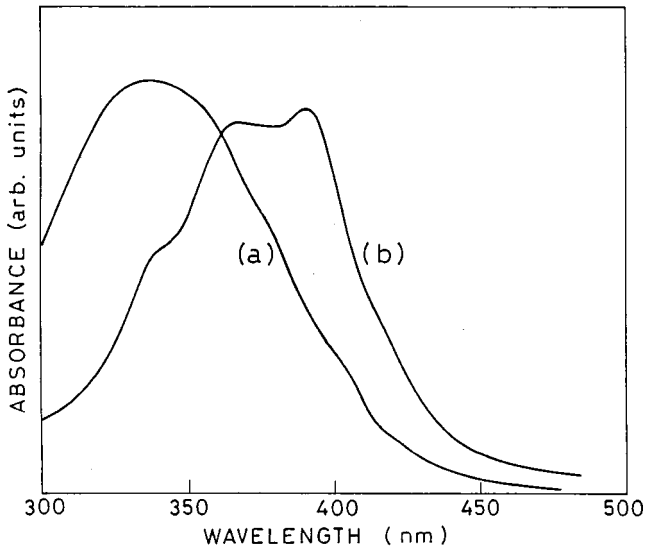

FIG. 9. Calculated absorption curves at RT using Eqs. (2) and (3) and the parameter values given in Tables II and III: (a) standard electropolymerized PPP sample; (b) improved PPP sample.

From Eq. (2) the band shape $I(\Omega)$ is determined by the different contributions coming from $I(\Omega,n)$, weighted by P_n, the double Gaussian distribution already shown in Refs. 1 and 2 and given in Eq. (3) for the sake of clarity:

$$P_n=\frac{1-G}{(2\pi\sigma_1)^{1/2}}\exp-\left(\frac{n-n_1}{2\sigma_1}\right)^2+\frac{G}{(2\pi\sigma_2)^{1/2}}\exp-\left(\frac{n-n_2}{2\sigma_2}\right)^2 \tag{3}$$

where n_1 and σ_1 are the values of the most probable segment lengths and the related dispersion of the distribution for $n=2-8$ (short oligomers), while n_2 and σ_2 are the parameters for the distribution with $n=9-15$ (intermediate length oligomers). G is the weight of the second distribution with respect to the first one.

In Figs. 9(a) and 9(b) we give the absorption band shapes calculated for two different sets of distribution parameters given in Table III, and by using the values given in Tables I and II. The band shapes reported there are in good agreement with the experimental data reported in Fig. 1. Note that while the values of n_1 and n_2 given in Table III for Figs. 9(a) and 9(b) are equal in both sets of parameters, the G value is different for the two bands shapes. In fact, the redshift of the band shape of Fig. 9(b) is well taken into account with a value of $G=0.7$, which means a higher contribution of intermediate length segments in $I(\Omega)$, with respect to the distribution used in Fig. 9(a).

TABLE III. Distribution parameters used in the calculations of absorption and Raman band shapes for different PPP samples.

	n_1	σ_1	n_2	σ_2	G
Figs. 9(a) and 11	11	1	8	2	0.5
Fig. 9(b)	11	1	8	2	0.7
Fig. 12	11	1	6	2	0.4

In order to evaluate the spectra of Raman scattering in resonance or in preresonance (RRS) conditions of PPP, we use the first-order RRS cross section $\alpha_f(\Omega_L,\omega)$, for each vibrational mode f, given in the equation.

$$\alpha_f(\Omega_L,\omega)\approx\sum_{n=2}^{15}|M_n|^4S_{f,n}\times\left|\sum_{l=0}^{l}(-)^lR_n(\Omega_L-l\omega_f)\right|^2 \times\frac{1}{\sqrt{2\pi\Delta_f}}\exp-\left(\frac{\omega-\omega_f}{2\Delta_f}\right)^2\times P_n, \tag{4}$$

where Ω_L is the laser excitation frequency ω is the frequency in the Stock range, Δ_f is the width of the Raman bands at ω_f, and P_n is the distribution given in Eq. (3). In this way, the first-order RRS spectra are calculated by summing up the contributions coming from different $\alpha_f(\Omega_L,\omega)$ for $f=1-3$. For the sake of clarity in the following equation we give $R_n(\Omega_L-l\omega_f)$ for $l=0$, already reported in Refs. 1 and 2 in order to show that this function is written in terms of the same physical quantities and parameters which enter into $I(\Omega,n)$ of Eq. (1):

$$R_n(\Omega_L)=\exp\left[-\sum_{f=1}^{3}S_{f,n}\right]\sum_{j=0}^{2}\sum_{f=1}^{3}\frac{(S_{f,n})^j}{(j)!} \times\frac{\gamma_n+i(\Omega_L-\Omega_n-j\omega_f)}{\gamma_n^2+(\Omega_L-\Omega_n-j\omega_f)^2}. \tag{5}$$

In Figs. 10(a) and 10(b), we report the calculated RRS band shapes for the three most intense vibrational modes considered for the oligomers Φ_4 and Φ_8, respectively, with $\lambda_L=676.4$ nm, while in Figs. 11(a)–11(c) we show the calculated RRS spectra of standard electropolymerized PPP at room temperature, obtained by using Eqs. (4) and (5), and by adding the different RRS cross sections $\alpha_f(\Omega_L,\omega)$ for $f=1-3$. The parameters used are given in Tables I–III, and in all the evaluations of Eq. (4) we have taken $\Delta_f=6\ \mathrm{cm}^{-1}$. The band shapes and intensities in the RRS spectra shown in Figs. 11 are calculated for $\lambda_L=676.4$, 363.8 and 351.1 nm, respectively. The change of I_{1280}/I_{1220}, going from the red to ultraviolet wavelength ranges, is in good agreement with the experimental data reported in Sec. II. In fact, from the calculated ratio we find an increase from 0.3 for $\lambda_L=676.4$ nm to 0.53 at $\lambda_L=351.1$ nm, due to improved resonance conditions with short conjugated segments (decreasing n). As we previously discussed, the electron vibration coupling with the mode at 1280 cm^{-1} increases in the shorter oligomers due to lower degree of planarity[20] of these systems. For decreasing n, on the contrary, the coupling with the mode at 1220 cm^{-1} decreases (see Table II). As a consequence, the ratio between the intensities of these two modes increases when λ_L is more in resonance with the electronic transitions of short conjugated segments. Also, the ratio I_{1600}/I_{1280} decreases when the laser light λ_L is tuned from the red to the ultraviolet frequency region due to the change of the resonance condition of the incident laser frequency with the electronic transitions of the oligomers. In fact, for decreasing n, the lower degree of planarity and the localiza-

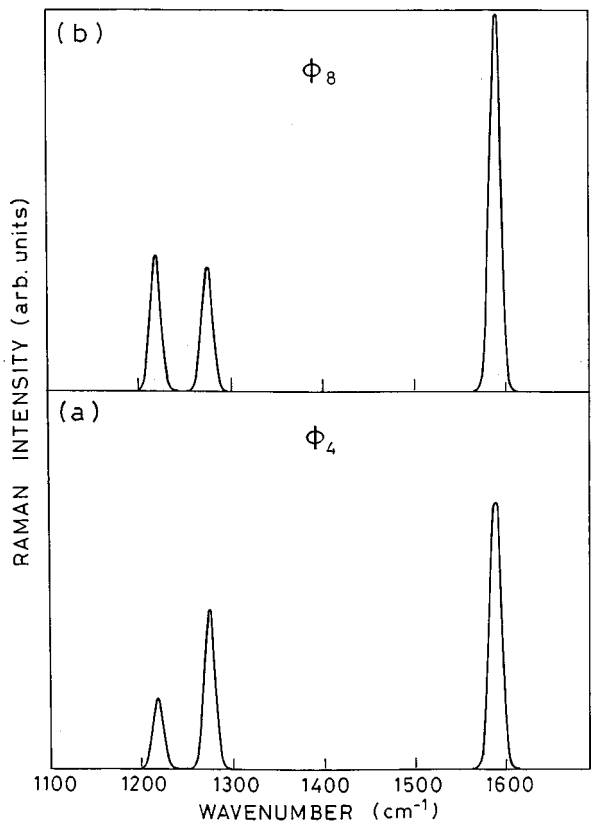

FIG. 10. Calculated Raman band shapes of the three most intense vibrational modes considered for the oligomers Φ_4 and Φ_8, with $\lambda_L = 676.4$ nm: (a) Φ_4 and (b) Φ_8. The parameter values are given in Table II.

tion of the excited states determine an increase of I_{1280} and a decrease of I_{1600}, with respect to the case of intermediate segment lengths. The changes of both ratios just discussed are a very important indication that a distribution of effective conjugated lengths simulates the standard electropolymerized PPP.

In order to corroborate this result, in Fig. 12 we show the RRS spectra of a sample of electropolymerized PPP simulated by distribution parameters given in Table III, for $\lambda_L = 676.4$ and 351.1 nm, respectively. While the spectrum at $\lambda_L = 676.4$ nm given in Fig. 12(a) is fairly similar to that of Fig. 11(a) ($I_{1280}/I_{1220} \sim 0.3$), a substantial difference is observed for $\lambda_L = 351.1$ nm in Fig. 12(b) with respect to the spectrum of Fig. 11(c). In fact, for the spectrum of Fig. 12(b) $I_{1280}/I_{1220} \sim 0.8$, while in Fig. 11(c) this ratio is 0.53. This drastic change of the ratio is due to a larger contribution of short oligomers with respect to the case of Fig. 11(c), which brings about an increase of I_{1280} with respect to I_{1220}. Conversely, for $\lambda_L = 676.4$ nm, the slight change of the intermediate conjugated segments, which mainly contribute to the RRS cross sections for this wavelength, cannot modify this ratio with respect to the case of Fig. 11(a). The spectrum shown in Fig. 12(b) has to be compared with that of Fig. 7(c), and the overall spectra given in Fig. 12 with those reported in Ref. 5

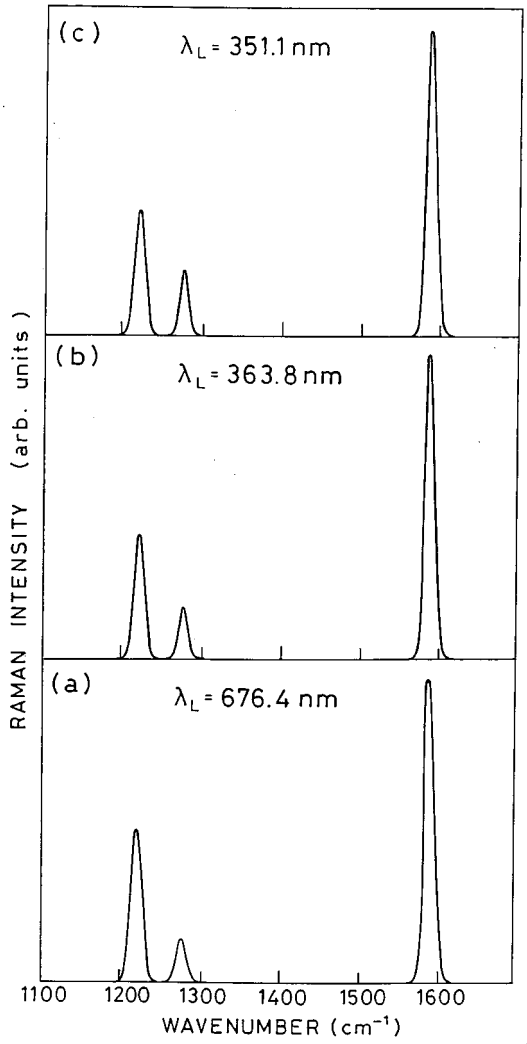

FIG. 11. Calculated Raman band shapes of the three most intense vibrational modes considered for the standard electropolymerized PPP using Eqs. (4) and (5) and the parameters given in Tables II and III: (a) $\lambda_L = 676.4$ nm, (b) $\lambda_L = 363.8$ nm, and (c) $\lambda_L = 351.1$ nm.

IV. DISCUSSION AND CONCLUSION

In this paper we have presented a systematic study of the optical properties of polyparaphenylene including optical absorption, photoluminescence, and Raman scattering, by extending to this polymeric compound the kind of investigation performed on PPV.[1] Note that studies on MEH-PPV were recently published in Ref. 21, in which the model rather similar to that of Ref. 1 was used to analyze the absorption and luminescence data.

The results given in this paper were accomplished by using the well-known properties of short oligomers Φ_2, Φ_3, and Φ_4, also including Φ_6 and Φ_8, which were synthesized in the Laboratoire of Physique Cristalline. We have carried out calculations of the optical features of PPP and its oligomers, which mainly consist of the simulations of the UV visible absorption band shapes and the Raman band intensities.

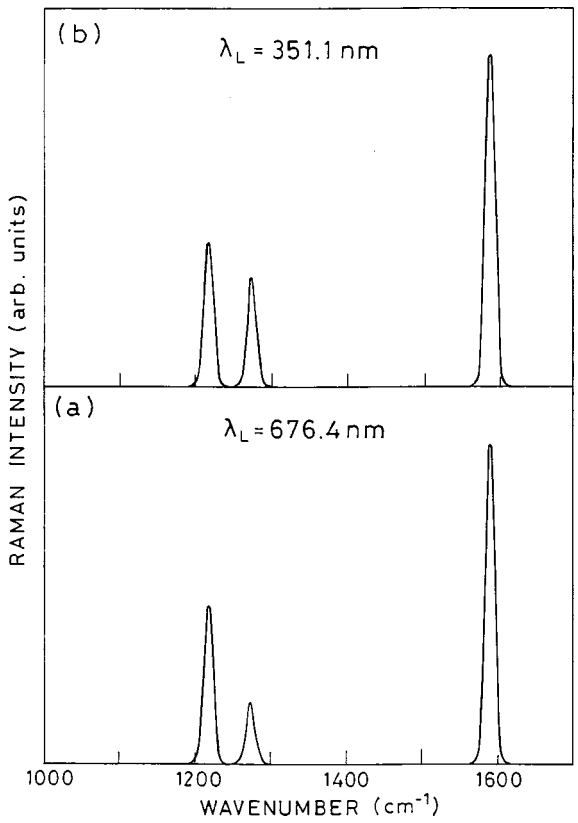

FIG. 12. Calculated Raman band shapes of electropolymerized PPP for the same modes as in Fig. 11, using the parameters given in Tables II and III: (a) $\lambda_L = 676.4$ nm and (b) $\lambda_L = 351.1$ nm.

The main result of this investigation is that the properties of PPP can be accounted for only if a distribution of conjugated segments lengths is introduced. As a matter of fact, we have shown that the absorption (band shape and peak position) and the intensity ratios of the main Raman bands are strongly dependent on such a distribution. We may emphasize that the intensity ratios measured at different excitation wavelengths from the near IR (1064 nm) to the near UV (351.1 nm) are a crucial probe in order to determine the composition of the material in terms of conjugated segments. In fact, in the red excitation wavelength range, from the intensity ratios one can determine the weight of the longest effective conjugation lengths present in the sample, while in the near-UV range one can test that of the shorter lengths (see Figs. 6 and 7). As an example, following the model proposed here, the electropolymerized PPP sample (standard and the one issued by different synthesis) is well described by a bimodal distribution centered on 11 and 8 phenyl rings, respectively (see Table III). Let us note that the change in the relative weight of these two distributions can describe the main features experimentally observed in both the absorption and Raman band relative intensities of PPP samples issued by different methods of synthesis.

According to this model it appears that luminescence spectra alone cannot be used as probes for the overall optical properties of the material, since the onset of the emission is determined by the longest conjugation lengths present in the sample. Only from the distribution obtained by an analysis of absorption and Raman scattering one can know which are the longest conjugated segments from where, most probably, the luminescence arises. Therefore, absorption and Raman scattering data at different resonant wavelengths are definitely needed in order to determine the distribution of the effective conjugation length, and in particular the longest ones in the distribution. From this study we may invoke the possibility of observing a mixture of effective conjugation lengths in some oligomers such as Φ_8 and Φ_6. It turns out that in the oriented Φ_6 oligomers, the intensity ratio I_{1280}/I_{1220} varies drastically as a function of the excitation wavelengths[11] from the red to the near UV ranges, indicating that effective conjugation lengths longer than Φ_6 are present. In addition, the absorption curves of Φ_8 clearly show that this mixture is present in this material, since different components are needed to deconvoluate the absorption bands.

ACKNOWLEDGMENT

The ''Institut des Matériaux de Nantes'' is Unité Mixte de Recherche No. 6502 CNRS/Université de Nantes.

[1] E. Mulazzi, A. Ripamonti, J. Wery, B. Dulieu, and S. Lefrant, Phys. Rev. B **60**, 16 519 (1999).
[2] G. P. Brivio and E. Mulazzi, Phys. Rev. B **30**, 876 (1984).
[3] E. Mulazzi, A. Ripamonti, T. Verdon, and S. Lefrant, Phys. Rev. B **45**, 9439 (1992).
[4] E. Mulazzi, A. Ripamonti, C. Godon, and S. Lefrant, Phys. Rev. B **57**, 15 328 (1998).
[5] J. P. Buisson, S. Krichene, and S. Lefrant, Synth. Met. **21**, 229 (1987).
[6] P. Kovacic and A. Kuriakis, J. Am. Chem. Soc. **85**, 454 (1963).
[7] T. Yamamoto, Y. Hayashi, and A. Yamamoto, Bull. Chem. Soc. Jpn. **51**, 2091 (1978).
[8] J. F. Fauvarque, A. Digua, M. A. Petit, and J. Savard, Makromol. Chem. **186**, 2415 (1985).
[9] G. Froyer, F. Maurice, J. Y. Goblot, J. F. Fauvarque, M. A. Petit, and A. Digna, Mol. Cryst. Liq. Cryst. **118**, 267 (1985).
[10] I. B. Berlam, *Handbook of Fluorescence Spectra of Aromatic Molecules* (Accademic, New York, 1965).
[11] L. Athouël, G. Froyer, M. T. Rou, and M. Shott, Thin Solid Films **274**, 35 (1996); L. Athouël, Ph.D. thesis, Université de Limoges (unpublished).
[12] S. Krichène, J. P. Buisson, and S. Lefrant, Synth. Met. **17**, 589 (1987); S. Krichène, Ph.D. thesis, Université de Nantes, 1986 (unpublished).
[13] D. Racovic, I. Bozovic, S. A. Shepanyan, and L. A. Gribow, Solid State Commun. **43**, 127 (1982).
[14] A. Bree and M. Edelson, Chem. Phys. Lett. **46**, 500 (1977).
[15] R. M. Barret and D. Steele, Spectrochim. Acta, Part A **30**, 1731 (1974).
[16] Y. Furukawa, H. Ohta, A. Sakamoto, and M. Tasumi, Spectro-

chim. Acta, Part A **47**, 1367 (1991).
[17] E. Burgos, H. Bonadeo, and E. D'Alessio, J. Chem. Phys. **65**, 2460 (1976).
[18] I. Bozovic and D. Rakovic, Phys. Rev. B **32**, 4235 (1985).
[19] G. Zannoni and G. Zerbi, J. Chem. Phys. **82**, 31 (1985).
[20] S. Guha, W. Graupner, S. Yang, M. Chandrasekhar, H. R. Chandrasekhar, and G. Leising, Phys. Status Solidi B **211**, 177 (1999).
[21] R. Chan, J. H. Hsu, W. S. Fann, K. K. Liang, C. H. Chang, M. Hayashi, J. Yu, S. H. Lin, E. C. Chang, K. R. Chuang, and S. A. Chen, Chem. Phys. Lett. **317**, 142 (2000).